Naval Research Laboratory

Washington, DC 20375-5320

NRL/MR/5650--06-8977

Modulation Diversity for Chromatic Dispersion Compensation in Analog Photonic Links

VINCENT J. URICK
FRANK BUCHOLTZ

Photonics Technology Branch
Optical Sciences Division

July 14, 2006

REPORT DOCUMENTATION PAGE

Form Approved
OMB No. 0704-0188

1. REPORT DATE *(DD-MM-YYYY)*	**2. REPORT TYPE**	**3. DATES COVERED** *(From - To)*
14-07-2006	Memorandum Report	April 25, 2004 - May 22, 2006

4. TITLE AND SUBTITLE

Modulation Diversity for Chromatic Dispersion Compensation in Analog Photonic Links

5a. CONTRACT NUMBER

5b. GRANT NUMBER

5c. PROGRAM ELEMENT NUMBER

6. AUTHOR(S)

Vincent J. Urick and Frank Bucholtz

5d. PROJECT NUMBER

5e. TASK NUMBER

5f. WORK UNIT NUMBER

7. PERFORMING ORGANIZATION NAME(S) AND ADDRESS(ES)

Naval Research Laboratory, Code 5652
4555 Overlook Avenue, SW
Washington, DC 20375-5320

8. PERFORMING ORGANIZATION REPORT NUMBER

NRL/MR/5650--06-8977

9. SPONSORING / MONITORING AGENCY NAME(S) AND ADDRESS(ES)

Office of Naval Research
One Liberty Center
875 North Randolph Street
Arlington, VA 22203-1995

10. SPONSOR / MONITOR'S ACRONYM(S)

ONR

11. SPONSOR / MONITOR'S REPORT NUMBER(S)

12. DISTRIBUTION / AVAILABILITY STATEMENT

Approved for public release; distribution is unlimited.

13. SUPPLEMENTARY NOTES

14. ABSTRACT

We present two solutions for chromatic dispersion compensation in analog photonic links based on modulation diversity. Both concepts are described in theory and demonstrated experimentally. The first, a modulation diversity transmitter, is shown to work only under specific conditions even though it intuitively seems the better solution. The modulation diversity receiver, on the other hand, is shown to be a completely passive device that adequately compensates for an arbitrary amount of chromatic dispersion in an analog fiber optic link. A band-limited design of the receiver is demonstrated, but essentially any bandwidth can be realized.

15. SUBJECT TERMS

Long haul fiber optic link
Analog photonics
Chromatic dispersion

16. SECURITY CLASSIFICATION OF:			**17. LIMITATION OF ABSTRACT**	**18. NUMBER OF PAGES**	**19a. NAME OF RESPONSIBLE PERSON**
a. REPORT	**b. ABSTRACT**	**c. THIS PAGE**			Vincent J. Urick
Unclassified	Unclassified	Unclassified	UL	18	**19b. TELEPHONE NUMBER** *(include area code)* (202) 767-9352

Standard Form 298 (Rev. 8-98)
Prescribed by ANSI Std. Z39.18

TABLE OF CONTENTS

MODULATION DIVERSITY FOR CHROMATIC DISPERSION COMPENSATION IN ANALOG PHOTONIC LINKS

EXECUTIVE SUMMARY

- This report demonstrates two methods for mitigating chromatic dispersion in analog photonic links, namely, a modulation-diversity transmitter and a modulation-diversity receiver.

- The modulation-diversity transmitter compensates chromatic dispersion penalties under prescribed conditions.

- The modulation-diversity receiver is shown to compensate an arbitrary amount of net chromatic dispersion for a phase-modulated or intensity-modulated analog photonic link.

- Presented in this report is a comprehensive theoretical and experimental investigation into the modulation-diversity transmitter and the modulation-diversity receiver concepts.

Manuscript approved May 31, 2006.

MODULATION DIVERSITY FOR CHROMATIC DISPERSION COMPENSATION IN ANALOG PHOTONIC LINKS

1 INTRODUCTION

Chromatic dispersion (CD) penalties in long (>km) analog photonic links become increasingly troublesome as the employed frequency bands move beyond the RF domain and into the microwave and millimeter-wave. For example, CD can generate frequency-dependent loss and nulls in the power spectrum [1]. In addition, second-order harmonics and second-order intermodulation distortion, which can dominate over third-order intermodulation distortion, are enhanced by CD in multi-octave systems [2]. Furthermore, fiber nonlinearites such as self-phase modulation and cross-phase modulation are enhanced by CD and can lead to significant power penalties, especially in multichannel links [2]-[4]. It is therefore essential to consider CD compensation for any high-performance analog link with a length greater than a few kilometers.

The penalties attributed to CD are traditionally viewed in terms of intensity-modulated (IM) analog systems. However, it has recently been demonstrated that phase modulation (ΦM) can improve the performance in analog [5] and radio-over fiber [6] links. Similarly, polarization modulation (PM) has been proposed for multi-channel systems [7] and suffers from CD penalties similar to those in IM links [8]. Here we will show that ΦM is likewise similar to IM and that there is a quadrature-type relation between the two formats. While PM is interesting and a potentially useful analog format, we restrict the discussion here to ΦM and IM, proposing solutions that mitigate CD for both an IM and ΦM analog link.

Previous CD compensation techniques are typically limited to IM systems in which the CD is fixed. For example, by using specialty fibers, one can achieve a low net dispersion for a fixed transmission distance [9],[10]. Such passive compensation techniques are only useful when one has control over the fiber deployment. For instance, in an antenna remoting application where the fiber is already deployed, the net CD can be high and this technique is useless. Other novel techniques are used for digital systems, where tunable compensation is achieved on the receive end of the link [11]-[13]. These techniques are typically adaptive, requiring complicated electronics and covering only certain values of CD. However, there exist analog applications where arbitrary and instantaneous CD compensation is desired and/or required. Such applications include adaptable fiber-optic network terminals and switched delay lines for radar applications. There are potential candidates to fulfill this role, such as single-sideband (SSB) modulation [14],[15]. However, SSB modulation is difficult to accomplish wideband, results in degraded RF efficiency, and can increase second-order distortions. Here, we propose modulation-diversity solutions that achieve compensation for any arbitrary value of CD. We demonstrate a passive single-octave system but show by simulation that multi-octave operation is achievable.

In Section II the deleterious effects that CD has on IM and ΦM links are derived and demonstrated. This leads to the intuitive conjecture that a modulation-diversity transmitter (MDTx) should flatten the spectral response for an analog link. This is only the case for specific prepared conditions as is described in Section III. In Section IV, however, a modulation-diversity receiver (MDRx) is proposed and demonstrated for 3-7 GHz and 13-17 GHz systems, with link lengths of 50 and 100 km using standard single-mode fiber (SMF) only. The MDRx is completely passive and requires no CD measurement electronics. The bandwidth is limited by system components and simulations show that a 6-94 GHz version of the receiver can be realized, regardless of the link length or CD. The results of the modulation-diversity concepts are then summarized in Section V.

2 CHROMATIC DISPERSION IN ANALOG PHOTONIC LINKS

The effects of CD on analog links are reviewed in terms of the direct-detection fundamental spectral response for both IM and ΦM formats. They are shown to be in quadrature with respect to RF power, which suggests a modulation diversity solution for CD mitigation.

2.1 Intensity Modulation

For an IM analog link, we employ an external balanced Mach-Zehnder modulator (MZM) biased at quadrature and direct detection with a p-i-n photodiode. This is the typical configuration for long high-performance analog links [1],[16]. The applied modulation at RF frequency $\Omega/2\pi$ is given by $\phi(t) = \pi/2 + \phi_0 \sin\Omega t$ where $\phi_0 = \pi\left(V_{rf}/V_\pi\right)$ with V_{rf} being the applied peak voltage and V_π the voltage required to yield π optical peak phase shift, a metric of the MZM. Given this modulation, the optical field at the output of the MZM can be written

$$E(z,t) = -q\sqrt{P_o}J_0\left(\frac{\phi_o}{2}\right)\sin(\omega_o t - \beta(\omega_o)z) - q\sqrt{P_o}\sum_{\substack{m=-\infty \\ m\neq 0 \\ m\,even}}^{\infty} J_m\left(\frac{\phi_0}{2}\right)\sin(\omega_o t + m\Omega t - \beta(\omega_o + m\Omega)z)$$
$$+ q\sqrt{P_o}\sum_{\substack{k=-\infty \\ k\,odd}}^{\infty} J_k\left(\frac{\phi_0}{2}\right)\cos(\omega_o t + k\Omega t - \beta(\omega_o + k\Omega)z) \tag{1}$$

where q is a constant relating optical field to optical power, P_o is the optical input power at frequency $\omega_o/2\pi$, J_n is the n^{th} order Bessel function of the first kind, and β_ν is the propagation constant at optical angular frequency ν. The mode-propagation constant can be expanded in a Taylor series as [17]

$$\beta(\omega) = \beta_o + \beta_1(\omega - \omega_o) + \frac{1}{2}\beta_2(\omega - \omega_o)^2 \tag{2}$$

where the commonly used dispersion parameter D is related to β_2, $D = -2\pi c\beta_2/\lambda^2$ with c being the speed of light in vacuum and λ the optical carrier wavelength. By inserting (2) into (1), the optical field after propagating a length L in fiber with dispersion parameter D can be obtained. From this field, an optical intensity can be calculated which is then linearly proportional to the photocurrent generated by an uncompressed p-i-n photodiode. This current is sourced to a load with impedance Z and the resulting frequency-dependent fundamental power is given by

$$P(\Omega) = \frac{1}{8}(\Re P_o\phi_0)^2 Z\cos^2\left(\frac{D\lambda^2 L\Omega^2}{4\pi c}\right) \tag{3}$$

where $\Re$ is the photodiode responsivity, the frequency response of the MZM and detector have been excluded, and small modulation depth ($\phi_0 << 1$) is assumed. Equation (3) is the commonly derived result [1] and, in the absence of CD ($D = 0$), is constant across frequency for a fixed drive voltage (neglecting the frequency dependence of V_π).

2.2 Phase Modulation

It is commonly known that direct detection of an optically-phase-modulated field will yield no RF photocurrent. This is simply because a photodiode responds to optical intensity and ΦM is a constant-intensity format. As will be shown, CD essentially rotates ΦM into IM resulting in a ΦM direct detection power response that is in quadrature with that for IM at the input.

With the same parameters as used previously, we have for the electric field at the output of an electro-optic phase modulator

$$E'(t) = q\sqrt{P_o}\sum_{n=-\infty}^{\infty} J_n(\phi_0')\cos\left[(\omega_o + n\Omega)t - \beta_{\omega_o+n\Omega}z\right] \tag{4}$$

where we establish the convention that primed variables correspond to ΦM and those umprimed correspond to IM or are arbitrary. Inserting (2) into (4) and using the same steps described earlier gives the ΦM direction-detection response as

$$P'(\Omega) = \frac{1}{2}\left(\Re P_o \phi_0'\right)^2 Z \sin^2\left(\frac{D\lambda^2 L\Omega^2}{4\pi c}\right) \tag{5}$$

The form of (5) predicts that the ΦM direct detection response is non-zero over frequency in the presence of net CD, thus suggesting that CD can "demodulate" a ΦM signal. While unconventional, this statement is correct in the sense that CD will transform ΦM information into IM information at some frequencies. This is in fact the goal of the demodulator for a ΦM system where typically some coherent [18] or interferometric [5],[6] approach is employed. A quantitative description of ΦM demodulation will be given in Section IV, as it is pertinent to the MDRx.

2.3 Comparison and Comments

The obvious relationship between the amplitude and phase modulation responses (3) and (5) is that they are in quadrature in the frequency domain. This is shown in Fig. 1, where the responses for an IM and ΦM direct-detection link are shown, as measured on a high-frequency network analyzer. For the data shown, the link length was 50 km , comprised entirely of SMF-28 (D = 17 ps/nm/km), and the transmitter wavelength was 1551 nm. The received DC photocurrent was 2.5 mA and the ΦM was padded to account for the amplitude mismatch and different modulator characteristics (insertion loss and V_π). It is precisely the complimentary relationship shown in Fig. 1 that leads to the proposition that modulation diversity should compensate for the effects of CD. For example, if an analog signal was launched with appropriate magnitudes of IM and ΦM, then direct detection at the receive end should result in a flat frequency response. Similarly, if either IM or ΦM were launched and both IM and ΦM were detected, the power response should be flat over the range of the ΦM detection technique. These are the two schemes that are explored in Sections III and IV.

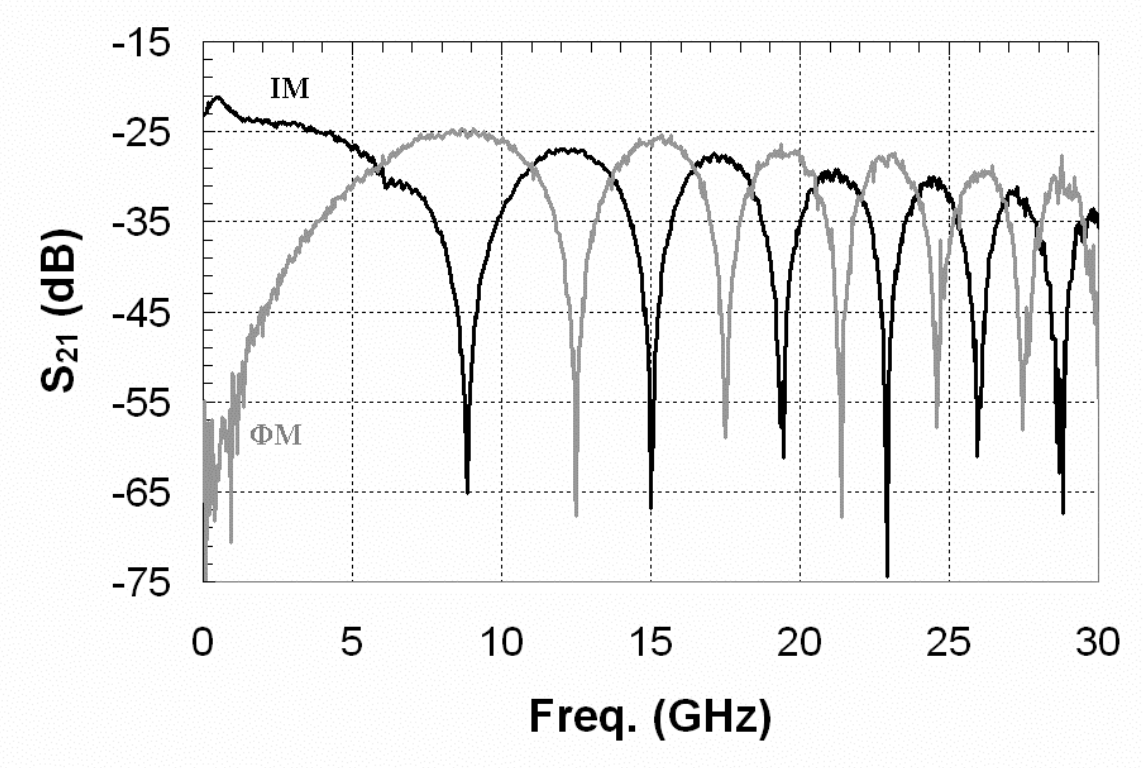

Fig. 1. Direct detection frequency response for IM (black) and ΦM (grey) after transmission through 50 km of SMF-28 fiber.

3 MODULATION-DIVERSITY TRANSMITTER

The architecture for the MDTx is shown in Fig. 2. The DFB semiconductor laser output is split into two paths using a polarization-maintaining fiber coupler. One path goes to a push-pull MZM biased at quadrature and the other to a phase modulator, with both modulators having polarization-maintaining fiber on their inputs and outputs. The input RF signal is split, weighted by RF pads, and modulated onto the phase and amplitude of the optical carrier. The output of the IM arm is rotated 90º before it is spliced to the polarization beam combiner, such that the two beams are combined in orthogonal polarizations. In addition, the ΦM path has a 500 m length (greater than the coherence length of the DFB) of polarization maintaining fiber to reduce interference effects, being that the polarization beam combiner has a finite extinction (~ 30 dB). This delay must be placed before the modulator because the RF paths from the signal input to the polarization beam splitter must be matched in true time. This results in IM and ΦM signals being launched from the MDTx, in orthogonal polarizations. Neglecting polarization-dependent loss (PDL) and polarization mode dispersion (PMD), a direct detection of the signal should result in a flat RF power response. This hypothesis results from the observations discussed in the previous section along with the assumption that the photodetector responds equally to both polarizations. To show that this is not exactly the case, we examine the MDTx theoretically and empirically.

To theoretically describe the MDTx, we assume no optical interference and that the RF path B→C in Fig. 2 is matched. Using (1) and (4), we can write the electric field at the MDTx output as a Jones vector:

$$\mathbf{E} = \left[\begin{array}{c} \left(-q\sqrt{P_o} J_0\left(\frac{\phi_o}{2}\right) \sin\left(\omega_o t - \beta(\omega_o) z\right) - q\sqrt{P_o} \sum_{\substack{m=-\infty \\ m\neq 0 \\ m\,even}}^{\infty} J_m\left(\frac{\phi_0}{2}\right) \sin\left(\omega_o t + m\Omega t - \beta(\omega_o + m\Omega) z\right) \right. \\ \left. + q\sqrt{P_o} \sum_{\substack{k=-\infty \\ k\,odd}}^{\infty} J_k\left(\frac{\phi_0}{2}\right) \cos\left(\omega_o t + k\Omega t - \beta(\omega_o + k\Omega) z\right) \right) \\ q\sqrt{2P_o} \sum_{n=-\infty}^{\infty} J_n(\phi_0') \cos\left[(\omega_o + n\Omega) t - \beta_{\omega_o + n\Omega} z\right] \end{array} \right] \tag{6}$$

Neglecting PDL and PMD, the field (6) propagates through a length $z = L$ and is incident on photodetector. Each polarization of the electric field creates a photocurrent that adds to give one net photocurrent. Assuming that there is equal small modulation depth in each polarization ($\phi_0 = 8\phi_0'$ and $\phi_0' << 1$) and that the detector responsivity is the same for both polarizations, the result for the RF power response is

$$P_{MDTx}(\Omega) = \frac{1}{4}\left(\Re P_o \phi_0'\right)^2 Z \left[1 - \sin\left(\frac{D\lambda^2 L\Omega^2}{2\pi c}\right)\right] \tag{7}$$

The response given by (7) is a periodic function that produces nulls and distortion! This result may seem counterintuitive but is explained as follows. While the two polarizations ideally propagate the fiber without interacting, the RF power that results from the two photocurrents has a mixing term, even for a path-matched system. In practice, small path imbalances in the path B→C can smooth out the response by adding additional interference terms to (7), much like an interleaver.

For experimental verification, the MDTx in Fig. 2 was constructed an evaluated in a 50 km link. The link is shown in Fig. 3 and consists of the MDTx, a 50 km span of SMF-28 fiber, and an Erbium-doped fiber amplifier (EDFA) at the output to compensate for link loss. For direct detection, a high-frequency p-i-n photodetector (Discovery Semiconductor DSC-20H) was used.

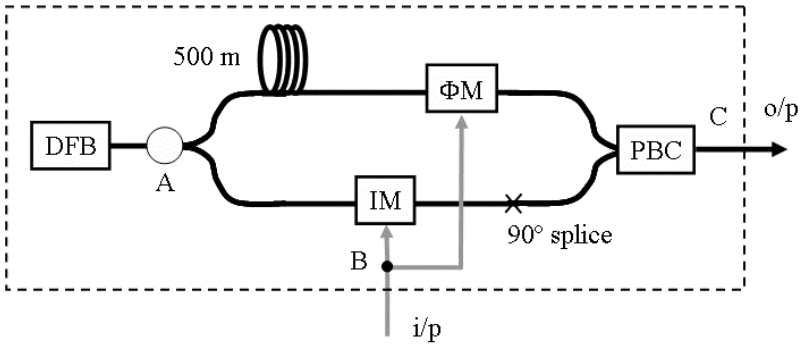

Fig. 2. The schematic for the modulation-diversity transmitter. DFB: distributed feedback semiconductor laser, ΦM: $LiNbO_3$ phase modulator, IM: $LiNbO_3$ MZM, PBC: polarization beam combiner. The optical path A→C is constructed using all polarization-maintaining components. The RF path B→C is matched in true time.

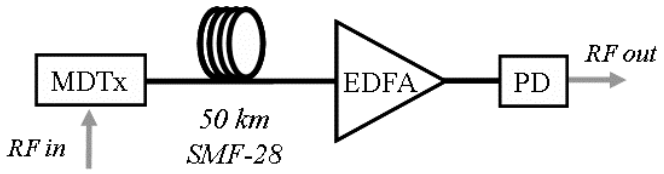

Fig. 3. Link used to evaluate the MDTx, as constructed in Fig. 2.

The results for this experiment are depicted in Fig. 4, showing the measured frequency responses for the path-matched MDTx and a path-imbalanced MDTx. For comparison, the IM response without the MDTx is also shown. For these data, the launch power into the link was +5 dBm and the EDFA optical gain was 16 dB, resulting in a received photocurrent of 5.5 mA. Note the periodic nulls in the path-matched MDTx response agree with (7) for λ = 1551 nm and D = 17 ps/nm/km. Short of shifting the nulls, the MDTx in this arrangement does not mitigate the effects of CD. However, for the path-imbalanced MDTx, the response is relatively flat to about 25 GHz, as compared to IM response. Ultimately, the path-imbalanced MDTx is not an adequate solution unless the considerable power ripple of more than 3 dB can be tolerated. Therefore, while interesting, the MDTx is not a complete solution for CD compensation in analog links. However its counterpart, the MDRx, does fill the role as is demonstrated in Section IV.

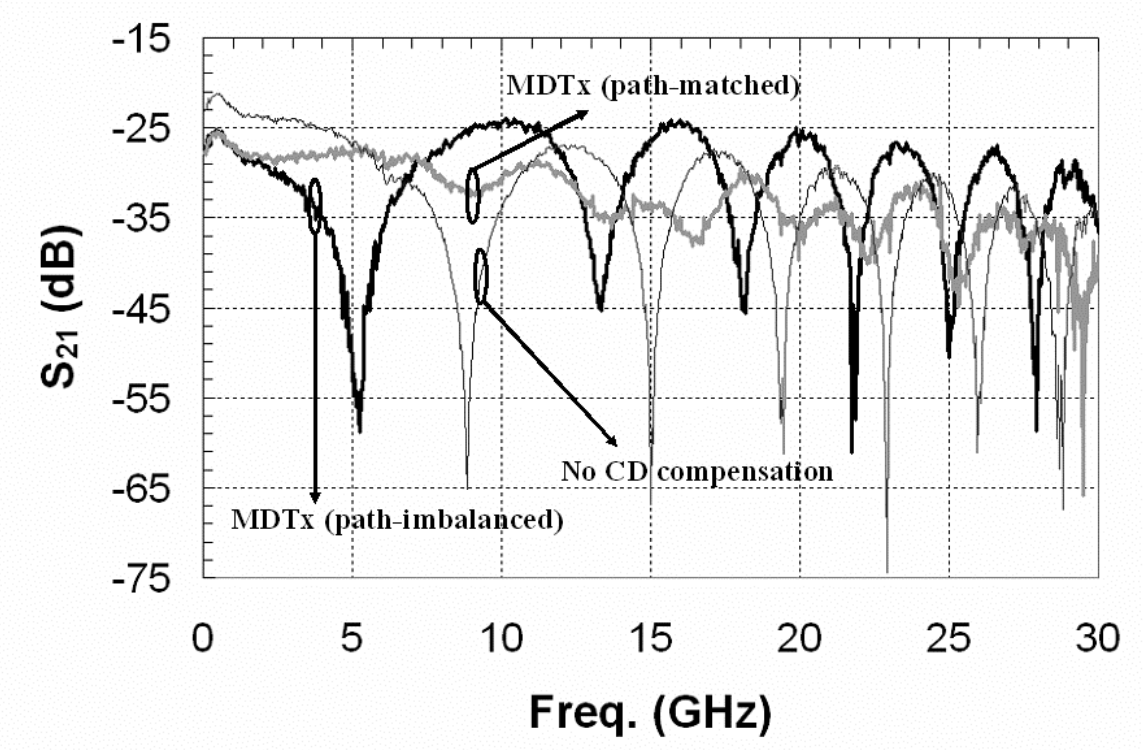

Fig. 4. Measured frequency response for the MDTx. Both the path-matched MDTx (dark black) and the path-imbalanced MDTx (grey) responses are shown, along with the IM response without the MDTx (light black) for comparison.

4 MODULATION-DIVERSITY RECEIVER

4.1 Analog Phase Demodulation

Before discussing the design and operation of the MDRx, it is instructive to review analog phase demodulation using an interferometer. It was noted in Section II that direct detection of a phase-modulated electric field (4) would result in no RF photocurrent in the absence of CD. A demodulation mechanism for analog ΦM is a path-imbalanced Mach-Zehnder interferometer (MZI) biased at quadrature. That is, for a given range of frequencies, the MZI rotates ΦM into IM such that direction detection yields an RF photocurrent. Furthermore, an MZI employing balanced detection responds to ΦM only and IM at the input produces no RF photocurrent. Quantitatively, we can model the two outputs of an MZI as

$$\begin{bmatrix} E_1(t) \\ E_2(t) \end{bmatrix} = \frac{1}{2}\begin{bmatrix} 1 & i \\ i & 1 \end{bmatrix}\begin{bmatrix} \Gamma(\tau) & 0 \\ 0 & 1 \end{bmatrix}\begin{bmatrix} 1 & i \\ i & 1 \end{bmatrix}\begin{bmatrix} E_{in}(t) \\ 0 \end{bmatrix} \tag{8}$$

where τ is the relative time delay between the two MZI paths, $\Gamma(\tau)$ is an operator that differentially delays one arm of the MZI by a time τ, and $\omega_o \tau = \pi/2$ at quadrature bias (note that (8) is not a Jones vector but rather a matrix representation of an MZI). Inserting (4) with $z = 0$ for $E_{in}(t)$ in (8), subtracting the photocurrents associated with $E_1(t)$ and $E_2(t)$ (balanced detection), and calculating the power response gives

$$P'_{MZI}(\Omega) = \frac{1}{2}(\Re P_o \phi'_0)^2 Z(1 - \cos\Omega\tau) \tag{9}$$

where it is again assumed that $\phi'_0 << 1$. Therefore, for the frequencies where $(1 - \cos\Omega\tau) \approx 2$, the

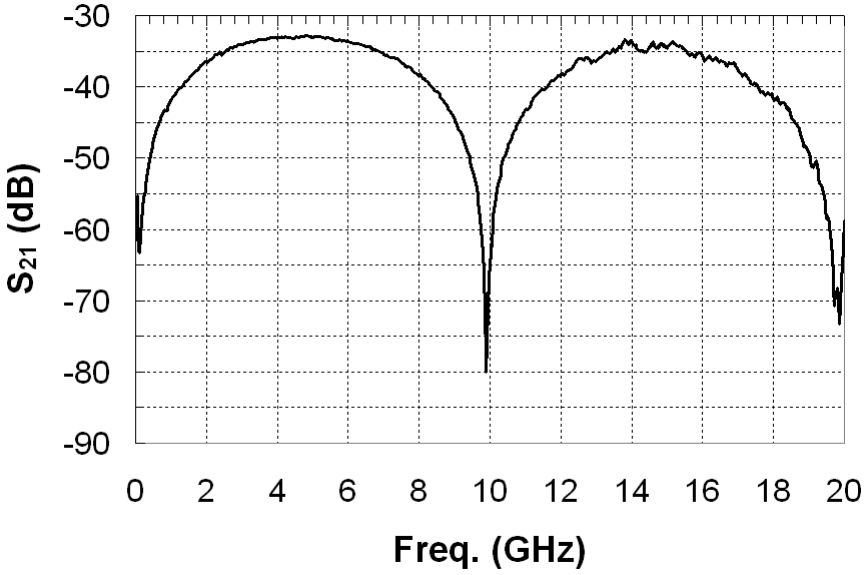

Fig. 5. Measured frequency response for a 100 ps differential delay MZI used as an analog ΦM demodulator.

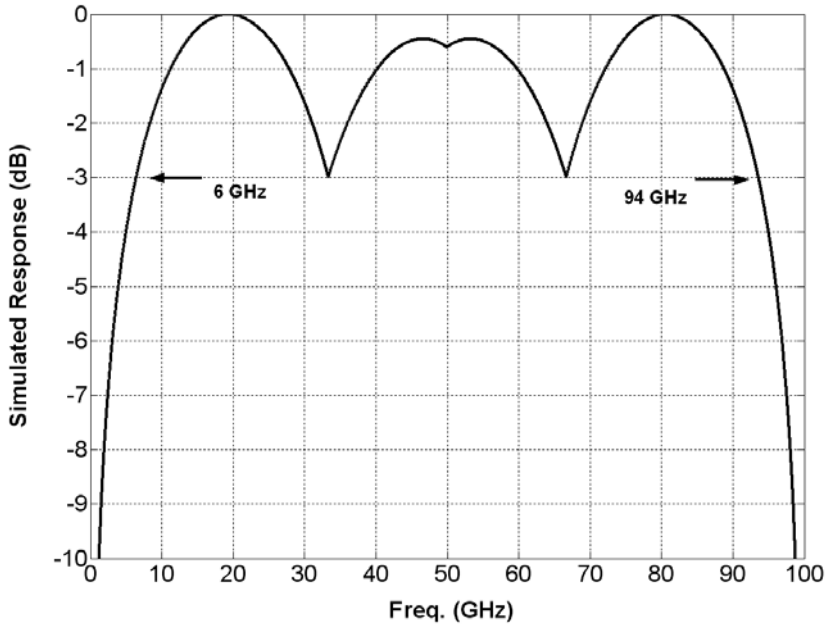

Fig. 6. Simulated response for three parallel MZI's (10, 20 and 30 ps delays) acting as analog ΦM demodulators.

ΦM is demodulated by the MZI. Note here that if (1) with $z = 0$ were used as $E_{in}(t)$, the resulting IM/balanced-detection MZI response would be $P_{MZI}(\Omega) = 0$. An example of the response given by (9) is shown in Fig. 5, where a commercially-available differential phase shift keyed demodulator with exceptional polarization stability (ITF Optical Technologies) was used to demodulate analog ΦM at its input. Here, $\tau = 100$ ps and no link was used such that the net CD was practically zero. We define the operation bandwidths of this MZI in terms of its analog 3-dB bandwidths, namely 3-7 and 13-17 GHz. It must be stressed that these bandwidths are determined completely by τ as given by (9). In fact, a parallel array of MZI's could cover much larger bandwidths, as shown in Fig. 6. Fig. 6 shows the simulated response of three parallel MZI's employing balanced detection with differential delays of 10, 20 and 30 ps. The normalized response shows a 3-dB bandwidth of 88 GHz (6-94 GHz) with a 3 dB ripple over the band. While this is not the optimum configuration, it is shown to make the argument that any frequency range can be covered, depending on the number of MZI's that are employed. The only exception is that the response (9) is always zero at DC, dictating that low frequency coverage is limited. Given this, the MDRx can be shown to work in principle using the 100 ps MZI as an analog ΦM demodulator.

4.2 MDRx Design and Demonstration

Section III described the shortcomings of launching analog information in simultaneous IM and ΦM formats for CD compensation. Here we describe the method of launching analog IM *or* ΦM and using a receiver that is sensitive to both in order to mitigate frequency response penalties caused by CD. The architecture of the MDRx is depicted in Fig. 7. The input to the MDRx is split into two paths using a fused fiber coupler. The upper path goes through an unbalanced MZI biased at quadrature using a balanced detection scheme; the lower path consists of a single photo-

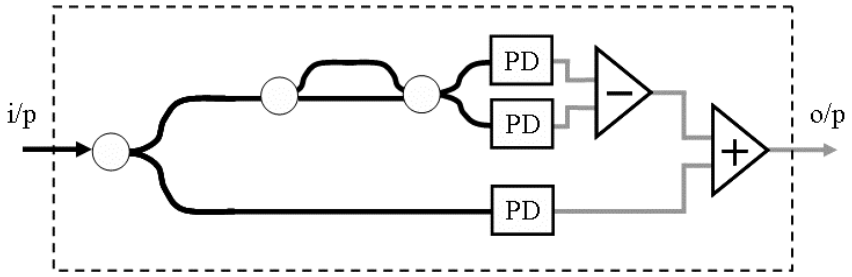

Fig. 7. The schematic for the MDRx. The upper arm of the receiver is sensitive to ΦM only; the lower arm is sensitive to IM only.

diode for direct detection. Therefore, the upper path is sensitive to ΦM only and the lower path is sensitive to IM only. The outputs are added in the RF domain using a 3-dB combiner, resulting in a total receiver output that contains contributions from both modulation formats. The upper and lower path must be matched within RF tolerances from the fiber coupler to the RF combiner to avoid RF interference.

To analyze the MDRx theoretically, we consider its power response when placed at the output of an IM or ΦM link. For IM, (1) is used with $z = L$ as the input field to the MDRx. The resulting power response is calculated as

$$P_{MDRx}(\Omega) = \frac{1}{8}(\Re P_o \phi_0)^2 \left[\cos^2\left(\frac{D\lambda^2 L\Omega^2}{4\pi c} \right) + (1-\cos\Omega\tau)\sin^2\left(\frac{D\lambda^2 L\Omega^2}{4\pi c} \right) \right] \tag{10}$$

The form of (10) intuitively makes sense. The first term, resulting from the lower path, is the IM-direct detection response as given by (3) having a squared-cosine dependence. The second term has the squared-sine dependence typical of the ΦM direct detection response (5) but weighted by the MZI response (9). Therefore, the upper path detects the IM that was rotated into ΦM by CD with the response governed by the MZI. For the frequencies at which $(1-\cos\Omega\tau) \approx 2$, the response (10) is independent of CD. That is, the response is flat over the frequency range for which the MZI demodulates ΦM. The ΦM response for the MDRx is obtained by using (4) as the input field:

$$P'_{MDRx}(\Omega) = \frac{1}{2}(\Re P_o \phi'_0)^2 \left[(1-\cos\Omega\tau)\cos^2\left(\frac{D\lambda^2 L\Omega^2}{4\pi c} \right) + \sin^2\left(\frac{D\lambda^2 L\Omega^2}{4\pi c} \right) \right] \tag{11}$$

where the second term is due to the lower path of the MDRx, the CD response for ΦM and direct detection. The first term is due to the upper path and quantifies the fact that the amount of ΦM at the output of the link follows squared-cosine dependence and is demodulated with the MZI response weighting. In summary, (10) and (11) describe how an analog signal, whether its initial modulation format was IM or ΦM, is rotated by CD into two quadrature components of IM and ΦM. These two components can be separately detected and recombined at the output of the link by using a receiver that is sensitive to IM and ΦM, such that all analog information is retained over the range that this detection can be implemented. This is precisely what the MDRx does in theory and, as will be shown, in practice.

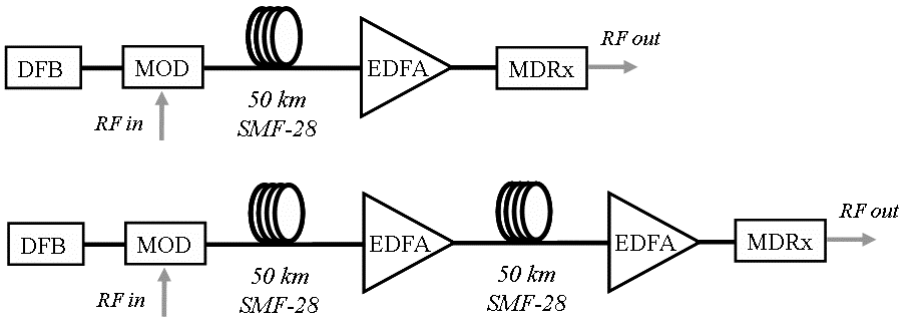

Fig. 8. 50 and 100 km links used for the demonstration of the MDRx.

The links used to demonstrate the operation of the MDRx are shown in Fig. 8. Four experiments were carried out: IM 50 and 100 km links, and ΦM 50 and 100 km links, all using SMF-28. For all experiments, a semiconductor DFB laser at 1551 nm used at the launch end and three 20 GHz p-i-n detectors (Discovery Semiconductor DSC-30S) were used to construct the MDRx. For both 50 km experiments, the detected DC current was 2 mA on all detectors. For both 100 km experiments, the DC current was 4 mA on all detectors. In each case, the EFDA gains were adjusted to compensate for link loss and the weighting of the upper and lower path of the MDRx was adjusted to ensure equal photocurrents on all detectors. The results of all four experiments are plotted in Fig. 9. In all cases, the effects of CD are compensated by the MDRx over the frequency ranges 3-7 and 13-17 GHz. Comparing either Figs. 9a and 9b or Figs. 9c and 9d demonstrate that the MDRx response does not depend on the net value of CD. Also, the subtleties of the above discussion are demonstrated, especially in Fig. 9d. Observe that there is a peak in the ΦM direct detection response near 14 GHz for the 100 km link. That is to say that at the output of the 100 km ΦM link, CD has transformed the ΦM into IM near 14 GHz. Furthermore, the ΦM MZI response for the same link has a null at that frequency, due the fact that the MZI responds to ΦM only. Finally, for that frequency with the MDRx, the information is recovered, albeit with some loss. This type of reasoning can be applied at any frequency for all of the graphs in Fig. 9 and lends to a deeper understanding of CD in an analog link.

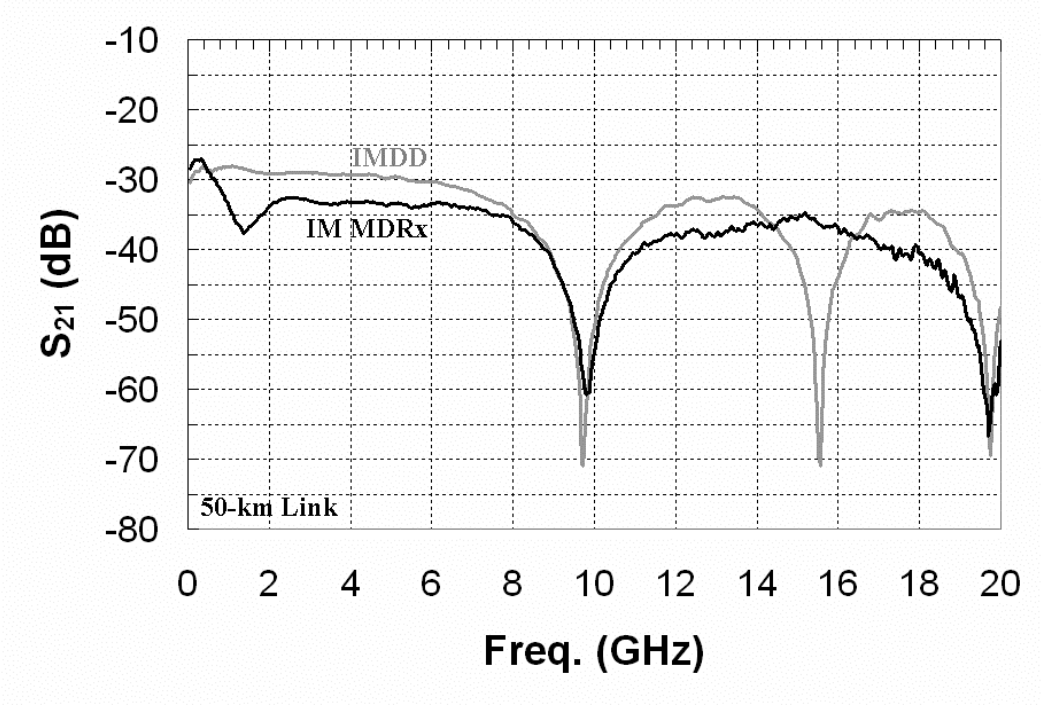
-10
-20
-30
-40
-50
-60
-70
-80
S21 (dB)
IMDD
IM MDRx
50-km Link
0
2
4
6
8
10
12
14
16
18
20
Freq. (GHz)

(a)

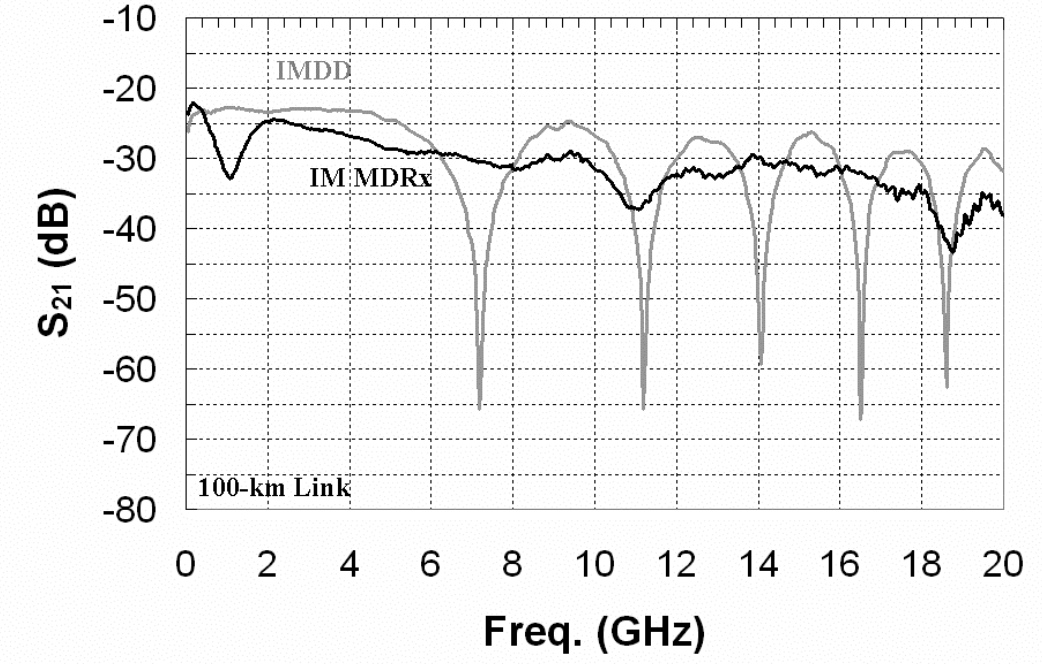
-10
-20
-30
-40
-50
-60
-70
-80
S21 (dB)
IMDD
IM MDRx
100-km Link
0
2
4
6
8
10
12
14
16
18
20
Freq. (GHz)

(b)

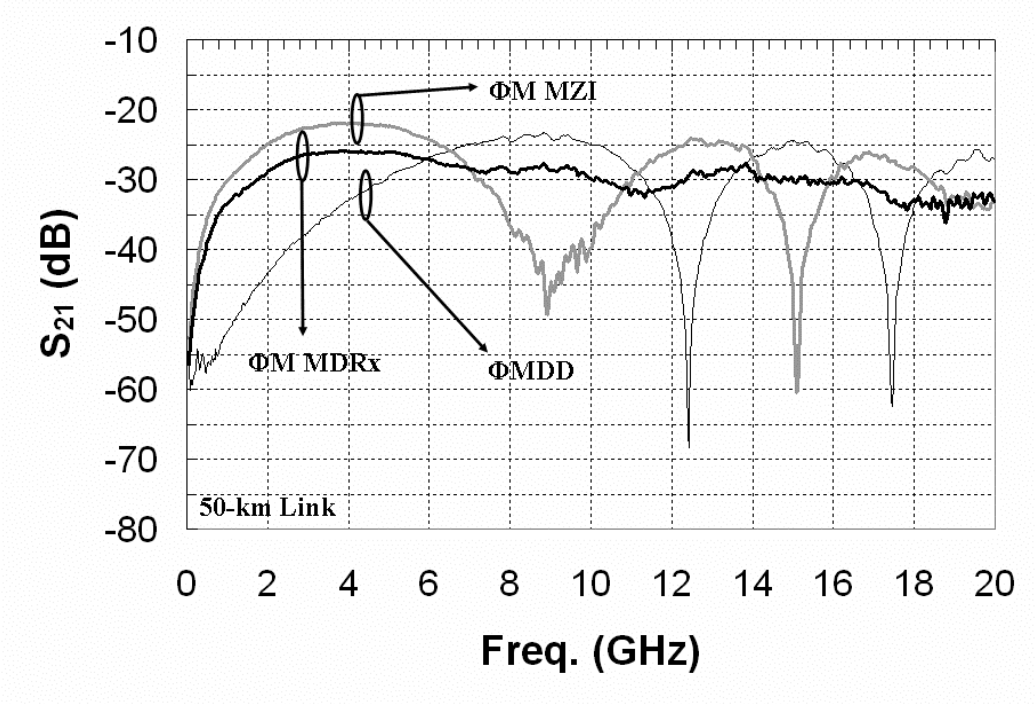

(c)

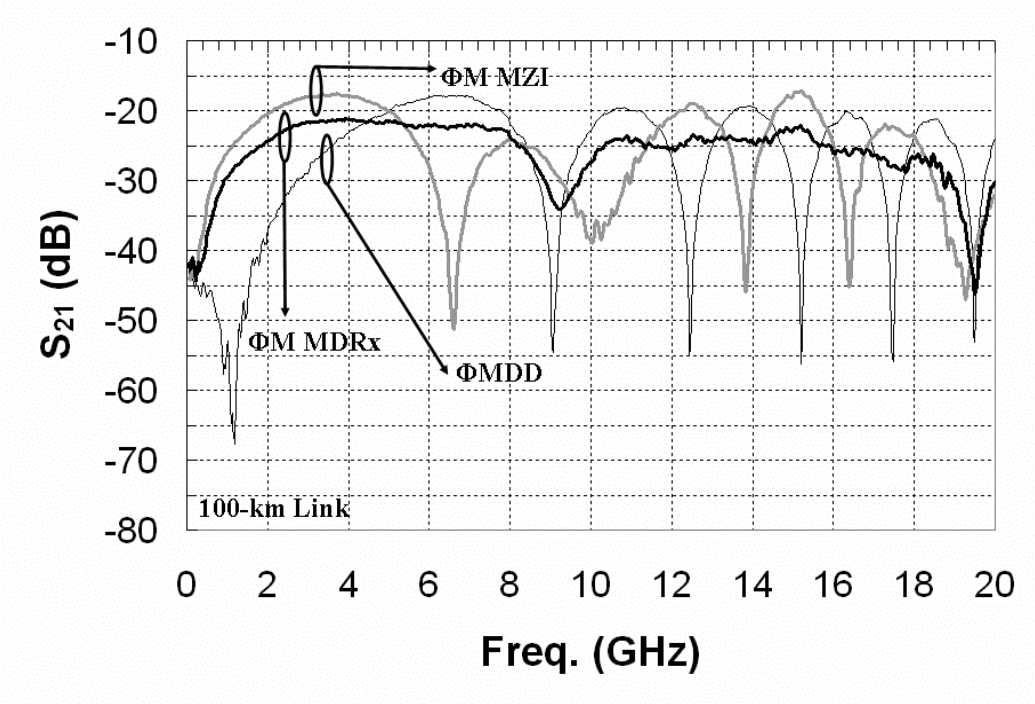

(d)

Fig. 9. Frequency responses for (a) 50 km IM link with MDRx (black) and with direct detection (grey); (b) 100 km IM link with MDRx (black) and with direct detection (grey); (c) 50 km ΦM link with MDRx (dark black), with direct detection (light black) and with MZI only (grey); (c) 100 km ΦM link with MDRx (dark black), with direct detection (light black) and with MZI only (grey).

5 SUMMARY AND CONCLUSIONS

Two solutions, based on modulation diversity, have been proposed and demonstrated for the mitigation of chromatic dispersion in analog links. The first, a modulation-diversity transmitter, does not completely compensate for the distortion caused by dispersion. It may, however, fill some niche for specific applications. The second solution, a modulation-diversity receiver, has been demonstrated in principle. It compensates for the power penalties induced by chromatic dispersion in an analog link employing either phase or amplitude modulation. The receiver works over any frequency range for which analog phase-modulation can be demodulated. We have demonstrated this receiver using a path-imbalanced Mach-Zehnder interferometer employing balanced detection but in practice, any phase-demodulation technique can be employed. However, the technique presented here is attractive because it is completely passive and requires only the electronics to bias the interferometer at quadrature. In addition, it does not depend on the value of the net chromatic dispersion, nor does it require chromatic dispersion measurement. Furthermore, the bandwidth of our technique can be increased significantly by employing a parallel array of interferometers, each with different delays. While this technique has been demonstrated for analog applications, it can be extended to digital signals whose pulse duration is shorter than the differential interferometer delay. Finally, we believe this work presents not only a solution to dispersion compensation but offers valuable insight into the effects of chromatic dispersion in analog photonic links.

ACKNOWLEDGMENTS

The authors wish to acknowledge Matthew Rogge, formerly an employee at the Naval Research Lab, for his valuable insight into the concept of a modulation-diversity transmitter.

REFERENCES

[1] H. Schmuck, "Comparison of optical millimeter-wave system concepts with regard to chromatic dispersion," *Electron. Lett.*, vol. 31, no. 21, pp. 1848-1849, Oct. 1995.
[2] E. E. Funk, A. L. Campillo, and D. A. Tulchinsky, "Nonlinear distortion and crosstalk in microwave fiber-radio links," in *IEEE MTT-S Digest*, vol. 3, pp. 1691-1693, June 2002.
[3] F. Bucholtz, V. J. Urick, and A. L. Campillo, "Comparison of crosstalk for amplitude and phase modulation in an analog fiber-optic link," in *Microwave Photonics Technical Digest*, Ogunquit, pp. 66-69, Oct. 2004.
[4] M. S. Rogge, V. J. Urick, F. Bucholtz, K. J. Williams, and P. Knapp, "Comparison of amplitude and phase modulation crosstalk in hyperfine WDM fiber optic links," in *CLEO/IQEC & PhAST Technical Digest*, Baltimore, paper CMH2, May 2005.
[5] V. J. Urick, F. Bucholtz, J. L. Dexter, K. J. Williams, and C. McDermitt, "Increased spurious-free dynamic range for an all-Raman 105 km link using phase modulation and balanced detection," in *CLEO/IQEC & PhAST Technical Digest*, San Francisco, paper CThBB1, May 2004.
[6] V. J. Urick, J. X. Qiu, and F. Bucholtz, "Wide-band QAM-over-fiber using phase modulation and interferometric demodulation," *IEEE Photonics Technol. Lett.*, vol. 16, no. 10, pp. 2374-2376, Oct. 2004.
[7] A. L. Campillo, F. Bucholtz, J. L. Dexter, and K. J. Williams, "Crosstalk reduction in wavelength division multiplexed analog links through polarization modulation," in *CLEO/IQEC & PhAST Technical Digest*, San Francisco, paper CWQ3, May 2004.

[8] A. L. Campillo, F. Bucholtz, and K. J. Williams, "Dispersion impairments in analog polarization modulated links," in *Microwave Photonics Technical Digest*, Ogunquit, pp. 104-106, Oct. 2004.
[9] H. Lu, "Performance comparison between DCF and RDF Dispersion compensation in fiber optical CATV systems," *IEEE Trans. on Broadcasting*, vol. 48, no. 4, pp. 370-373, Dec. 2002.
[10] V. J. Urick, J. X. Qiu, F. Bucholtz, C. McDermitt, and K. J. Williams, "4 Gbit/s transmission over single-channel Raman-amplified 105 km link," *Electron. Lett.*, vol. 40, pp. 495-496, Apr. 2004.
[11] Z. Pan, Y. W. Song, C. Yu, Y. Wang, Q. Yu, J. Popelek, H. Li, and A. E. Willner, "Tunable chromatic dispersion compensation in 40-Gb/s systems using nonlinearly chirped fiber Bragg gratings," *J. Lightwave Technol.*, vol. 20, no. 12, pp. 2239-2246, Dec. 2002.
[12] J. P. Weem, P. Kirkpatrick, and J. Verdiell, "Electronic dispersion compensation for 10 Gigabit communication links over FDDI legacy multimode fiber," in *OFC Technical Digest*, Anaheim, paper OFO4, March 2005.
[13] A. H. Gnauck, J. Sinsky, P. J. Winser, and S. Chandrasekhar, "Linear microwave-domain dispersion compensation of 10-Gb/s signals using heterodyne detection," in *OFC Post Deadline Papers*, Anaheim, paper PDP31, March 2005.
[14] G. H. Smith, D. Novak and Z. Ahmed, "Technique for optical SSB generation to overcome dispersion penalties in fibre-radio systems;" *Electron. Lett.*, vol. 33, no. 1, pp. 74-75, Jan. 1997.
[15] M. Sieben, J. Conradi, and D. E. Dodds, "Optical single sideband transmission at 10 Gb/s using only electrical dispersion compensation," *J. Lightwave Technol.*, vol. 17, no. 10, pp. 1742-1749, Oct. 1999.
[16] E. E. Funk, V. J. Urick, S. J. Strutz, J. L. Dexter, and K. J. Williams, "110 km 256-QAM digital microwave over fiber link," in *IEEE MTT-S Digest*, Philadelphia, pp. 269-272, June 2003.
[17] G. P. Agrawal, "Nonlinear fiber optics," 3rd ed., San Diego: Academic Press, 2001, pp. 7-13.
[18] A. Madjar, "Performance prediction and optimization of a coherent phase modulated low noise analog optical link operating at microwave frequencies," *IEEE Trans. Microwave Theory Tech.*, vol. 42, no. 5, pp. 801-806, May 1994.